Extracellular Biopolymer Production by *Acrostalagmus luteoalbus* from Agro-Industrial Wastes: Toward Sustainable Material Development

Raquel Gómez-Pliego *, Jair Alejandro Temis-Cortina, Karla Aidee Aguayo-Cerón, Hulme Ríos-Guerra, Harold Alexis Prada-Ramírez, Rodrigo Romero-Nava, Alfredo Briones-Aranda

Posted Date: 3 June 2026

doi: 10.20944/preprints202606.0282.v1

Keywords: biopolymer production; agro-industrial residues; *Acrostalagmus luteoalbus*; extracellular biopolymers; fungal biopolymers

 doi:10.20944/preprints202606.0282.v1

Article

Extracellular Biopolymer Production by *Acrostalagmus luteoalbus* from Agro-Industrial Wastes: Toward Sustainable Material Development

Raquel Gómez-Pliego [1,*], Jair Alejandro Temis-Cortina [1], Karla Aidee Aguayo-Cerón [2], Hulme Ríos-Guerra [3], Harold Alexis Prada-Ramírez [4], Rodrigo Romero-Nava [2] and Alfredo Briones-Aranda [5]

[1] Departamento de Ciencias Biológicas, Sección de Ciencias de la Salud Humana, Laboratorio de Microbiología Industrial, Facultad de Estudios Superiores Cuautitlán, Campo 1, Universidad Nacional Autónoma de México, Av. 1 de Mayo S/N, Santa María Guadalupe Las Torres, Cuautitlán Izcalli, C.P. 54740, Estado de México, México

[2] Laboratorio de Investigación en Genética de Enfermedades Metabólicas, Escuela Superior de Medicina, Instituto Politécnico Nacional, Plan de San Luis y Díaz Mirón S/N, C.P. 11340, Ciudad de México, México

[3] Departamento, de Ciencias Químicas, Sección de Química Orgánica, Laboratorio de Química Orgánica Multicomponente, Facultad de Estudios Superiores Cuautitlán, Campo 1, Universidad Nacional Autónoma de México, Av. 1 de Mayo S/N, Santa María Guadalupe Las Torres, Cuautitlán Izcalli, C.P. 54740, Estado de México, México

[4] Universidad de los Andes, Carrera 1 No.18A - 12. Cundinamarca, Bogotá, Colombia

[5] Laboratorio de Farmacología, Facultad de Medicina Humana,Universidad Autónoma de Chiapas, Décima Sur, esquina con calle Central s/n, C.P. 29000, Tuxtla Gutiérrez, Chiapas, México

* Correspondence: pliegoraquel@comunidad.unam.mx; Tel.: +52-55-56-23-20-04

Abstract

Microbial biopolymers produced from low-cost agro-industrial residues represent a promising alternative to persistent petroleum-derived plastics. In this study, the filamentous fungus *Acrostalagmus luteoalbus*, isolated from the beetle *Ulomoides dermestoides*, was evaluated for its ability to synthesize extracellular biopolymeric material using waste-derived carbon sources. To the best of our knowledge, no previous reports have described the production of extracellular biopolymers by *A. luteoalbus*. Biopolymer accumulation at the culture surface was monitored for up to eleven weeks using fruit-derived residues, with sucrose employed as a reference substrate. Substrate-to-product conversion yields showed a strong dependence on carbon source composition, with the highest value obtained using pulp with *Crataegus mexicana* (tejocote) peel (≈17.10 ± 1.29% at week nine), followed by sucrose-based media. The recovered material was dark brown, brittle, and insoluble in common polar and non-polar solvents, and exhibited a compact, heterogeneous surface morphology under scanning electron microscopy. Elemental (CHNS) analysis indicated a carbon-rich, nitrogen-poor composition, while thermogravimetric and calorimetric analyses revealed multistep thermal degradation with major mass-loss events occurring above 250 °C, consistent with a thermally stable polymeric material. These results demonstrate that *A. luteoalbus* can convert diverse agro-industrial residues into extracellular biopolymeric material under simple culture conditions. Although the detailed monomeric composition of the material remains to be elucidated, this work provides an initial physicochemical and thermal characterization that expands current knowledge of fungal biopolymer-producing systems and supports further investigation of this species as an alternative microbial platform.

Keywords: biopolymer production; agro-industrial residues; *Acrostalagmus luteoalbus*; extracellular biopolymers; fungal biopolymers

 doi:10.20944/preprints202606.0282.v1

1. Introduction

The large-scale synthesis and widespread use of synthetic polymers transformed modern society in the mid-20th century. Owing to their versatility, low cost, low density, and durability, plastics became essential for packaging, textiles, construction, automotive components, and consumer goods [1]. However, the combination of intensive global production, extended service life, and inadequate end-of-life management has resulted in an unprecedented accumulation of plastic residues in terrestrial and aquatic environments [2].

Global plastic production increased from about 2 million tons in 1950 to approximately 460 million tonnes in 2019, and annual plastic waste generation reached 353 million tonnes in the same year [3,4]. A substantial share of this waste is mismanaged, allowing it to disperse into soils, rivers, and marine ecosystems [4]. It is estimated that 19–23 million tonnes of plastic waste enter aquatic ecosystems annually [2]. Once released into the environment, plastics progressively fragment through mechanical abrasion, UV exposure, and oxidative processes, producing micro- and nanoplastics that can enter food webs and disrupt ecosystem functioning [5,6]. In addition, inadequate disposal practices, particularly uncontrolled burning of plastic-rich waste streams, contribute to the release of toxic compounds such as dioxins and furans [7].

Current evidence indicates that many commodity plastics degrade extremely slowly under environmental conditions, with residence times spanning decades to centuries, depending on polymer chemistry, formulation, and exposure regime [8,9]. In this context, there is growing interest in bio-based and biodegradable polymers as sustainable alternatives to conventional petrochemical plastics [10]. These materials are typically derived, at least in part, from renewable feedstocks (e.g., crops, lignocellulosic biomass, algae, or microbial cultures) and are often designed to biodegrade under defined conditions [11,12]. When integrated into circular value chains (reuse, composting, anaerobic digestion, and organic recycling), bioplastics may reduce dependence on fossil fuels and help close carbon cycles [13,14].

Polymer biodegradation involves microbial cleavage of macromolecular chains, ultimately leading to mineralization into CO_2, water, and biomass under aerobic conditions, or into CH_4 and CO_2 under anaerobic conditions [15]. These biotic processes frequently act in concert with abiotic mechanisms, including hydrolysis, thermal degradation, and photo-oxidation, whose relative contributions depend on the polymer's chemical structure, morphology, and environmental context [15,16]. Biopolymers can be broadly grouped into four categories: (i) naturally occurring renewable polymers, such as starch, cellulose, and chitin; (ii) microbial polymers, including polyhydroxyalkanoates (PHAs); (iii) chemically synthesized polymers derived from renewable monomers, such as polylactic acid (PLA); and (iv) biodegradable polymers of petrochemical origin, such as poly(ε-caprolactone) (PCL) [12,17]. Among these, PHAs, including poly(3-hydroxybutyrate) (PHB), have been extensively studied as biodegradable thermoplastics, with growing emphasis on lignocellulosic biomass and agro-industrial residues as low-cost feedstocks [18–20]. Nevertheless, industrial deployment remains constrained by high production costs, suboptimal yields, and energy-intensive downstream processing [19,21].

Most research on microbial biopolymers has focused on bacteria [22], whereas filamentous fungi remain comparatively underexplored as producers of PHA-like materials and extracellular polymeric substances [23]. Filamentous fungi exhibit high metabolic plasticity, strong secretory capacity, and the ability to grow on complex, heterogeneous substrates, supporting their potential for waste valorization [24,25]. In parallel, Selvam et al. (2025) highlighted agricultural wastes such as sugarcane bagasse, rice husks, banana peels, and spent mushroom substrate as suitable substrates; Jørgensen et al. (2007) discussed enzymatic conversion of lignocellulose into fermentable sugars; and Barua et al. (2025) summarized advances in converting lignocellulosic wastes into bioplastic precursors within circular bioeconomic frameworks [26–28]. Bio-based polymers have been applied in packaging, disposable items, textiles, agriculture, and biomedical materials (e.g., sutures, scaffolds, and drug-delivery systems) [11,29]. However, no single microbial biopolymer currently matches the combined mechanical, thermal, and processing performance of high-volume petrochemical plastics such as

 doi:10.20944/preprints202606.0282.v1

polyethylene, polypropylene, or PET, and key challenges remain in durability, stability, controlled degradation, and cost competitiveness [16,17].

The fungal genus *Acrostalagmus* is recognized for metabolic versatility and the production of structurally diverse natural products, including antimicrobial and cytotoxic metabolites [30]. *Acrostalagmus luteoalbus* has been reported in damp indoor environments and in contaminated building materials [31]; however, its capacity to synthesize extracellular biopolymers of technological relevance has not been reported previously. In particular, the chemical composition and monomeric building blocks of any polymeric materials potentially produced by this species remain unknown.

The present study addresses this knowledge gap by isolating *A. luteoalbus* from the insect *Ulomoides dermestoides*, a previously unexplored ecological niche for fungal biopolymer production. We evaluated its ability to produce extracellular biopolymers from agro-industrial residues, including orange peel, corn cob, banana peel, prickly pear peel, and pulp, using *Crataegus mexicana* (tejocote) peel as the carbon source, with sucrose as a reference substrate. The resulting materials were characterized in terms of physicochemical and thermal properties, including elemental composition, morphology, and thermal stability, providing an initial framework for future studies aimed at elucidating monomeric composition, structure–property relationships, and potential application domains.

2. Materials and Methods

2.1. Isolation and Molecular Identification of the Microorganism

2.1.1. Isolation of the Microorganism

Acrostalagmus luteoalbus was isolated from the beetle *U. dermestoides*, purchased from a specialized pet store in Mexico City, Mexico. To reduce potential contaminants associated with the insect's surface microbiota, six successive passages of the beetle culture were performed on chopped apple substrate that had been pasteurized (80 °C, 10 min). At each passage, beetles were allowed to reproduce, and neonate larvae were transferred to fresh pasteurized substrate. This procedure served as an *in vivo* biological decontamination step. By transferring only neonate larvae to fresh pasteurized substrate over six generations, the transient environmental microbiota associated with the insect's cuticle and gut was minimized, ensuring that the isolated fungi were true residents of the *U. dermestoides* microbiome.

Final isolation was performed using a homogenization and serial dilution method. Under sterile conditions, 10 g of adult beetles from the sixth generation were randomly selected, weighed, and macerated in a sterile mortar. The homogenate was suspended in 90 mL of sterile isotonic saline solution. After sedimentation of solids, serial dilutions (10^{-1} to 10^{-5}) were prepared. The final two dilutions were plated in triplicate on Potato Dextrose Agar (PDA) and Sabouraud Dextrose Agar (SDA) and incubated at 28 ± 0.5 °C for 7 days. A predominant fungal colony exhibiting a distinct macroscopic morphology was visually selected, isolated, and purified by repeated subculturing onto fresh PDA plates until an axenic culture was obtained.

2.1.2. Molecular Identification and Sequence Analysis

Molecular identification of the isolate was confirmed by amplification and sequencing of the internal transcribed spacer (ITS1–5.8S–ITS2) region using primers ITS5 and ITS4. The obtained sequence showed 100% identity with the reference strain *A. luteoalbus* (GenBank accession no. KT715723) based on BLASTn analysis. Identification was considered confirmed based on full-length ITS-region similarity. The strain is maintained at the Industrial Microbiology Laboratory, FESC-UNAM, Mexico.

 doi:10.20944/preprints202606.0282.v1

2.1.3. Nucleotide Sequence Accession Number

The ITS nucleotide sequence generated in this study was deposited in GenBank under accession number PX916169.1.

2.2. Formulation of Culture Media for Biopolymer Production

2.2.1. Carbon Sources and Medium Composition

Agro-industrial residues were used as carbon sources: orange peel, prickly pear peel, banana peel, corn cob, and tejocote (*Crataegus mexicana*) pulp with peel. Six solid culture media (wet basis) were formulated. Organic substrates (dry mass of milled residue) were adjusted to 50 g/L, except for *C. mexicana* pulp/peel (30 g/L). Sucrose (30 g/L) was used as the carbon source in the control medium to provide a highly assimilable and structurally simple baseline for accurate kinetic and yield comparisons. All agro-industrial substrates were previously hydrolyzed.

All media were supplemented with a mineral salts solution containing (g/L): $NaNO_3$ (3.0), KH_2PO_4 (1.0), $MgSO_4$ (0.5), KCl (0.5), and $FeSO_4$ (10 mg/L), and folic acid (0.166 g/L; vitamin B9) as an organic growth factor based on previous submerged-culture optimization studies, in which it showed the highest stimulatory effect on exopolysaccharide (EPS) production among the vitamins evaluated [32]. Bacteriological agar (15 g/L) was used as the gelling agent. All chemicals were analytical grade (Sigma-Aldrich), and culture media and microbiological components were obtained from Becton, Dickinson, and Company.

2.2.2. Substrate Pretreatment and Hydrolysis

Organic residues were washed, dried, and milled. To release basic fermentable sugars for culture media formulation, the substrates underwent a single-step dilute acid hydrolysis in an autoclave operated at reduced pressure (0.07 MPa; ≈115 °C) for 20 min, using the substrate concentrations described in Section 2.2.1. The pH was adjusted to 3.0 with 0.1 N HCl. The hydrolysates were treated with activated carbon to remove growth-inhibitory compounds generated during hydrolysis, then filtered through medium-porosity filter paper to remove suspended solids. The supernatants were collected and used to prepare culture media for biopolymer production

2.2.3. Preparation of Biopolymer Production Media

The hydrolyzed supernatant was mixed with the mineral salt solution, folic acid, and agar at the previously described concentrations. The final pH was adjusted to ≈ 6.0–6.5 by adding 1.0 N NaOH to maintain the medium within a range reported to favor the growth of *A. luteoalbus*, while simultaneously preventing excessive acidity that could intensify pH-dependent inhibition, characteristic of acid hydrolysates [33]. Subsequently, the medium was heated to a gentle boil to ensure complete dissolution of agar (visual clarification) and sterilized by autoclaving at 0.1 MPa (121 °C) for 15 min. Finally, the media were cooled to 50 ± 2 °C and poured into sterile Petri dishes (35 ± 1 mL per plate).

2.3. Biopolymer Production and Yield Evaluation

Petri dishes were inoculated with *A. luteoalbus* via stab culture and incubated at 28 ± 2 °C under aerobic conditions. Production kinetics were monitored weekly for 11 weeks via destructive sampling, sacrificing triplicate Petri dishes each week to determine the dry weight of the recovered biopolymer, thereby allowing us to obtain the complete biopolymer production profile and to identify the onset of the production plateau. The extended incubation period was selected based on the slow, progressive accumulation of extracellular polymeric material at the air–medium interface, a characteristic of filamentous fungal growth on solid substrates and not adequately captured in short-term fermentations. This approach also allowed verification that polymer accumulation

 doi:10.20944/preprints202606.0282.v1

remained stable over time and was not followed by detectable degradation due to nutrient depletion. All experiments were performed in triplicate.

For extraction, because the biopolymer is secreted as a distinct extracellular layer at the air–medium interface, it was visually identified and physically separated from the underlying vegetative mycelium before collection. The collected polymeric material was subjected to thermal treatment (0.1 MPa, 121 °C, 30 min) to solubilize any remaining agar matrix and release the biopolymer. This processing temperature (121 °C) is well below the onset degradation temperature (T_0) reported for fungal polysaccharides and cellulosic materials, which typically exceeds 200–250 °C [34]. Therefore, this method enables efficient recovery of the material without inducing thermal degradation, as confirmed by TGA analysis (Section 3.2)

The recovered biopolymer was purified by refluxing in distilled water for 3 h to remove unassimilated water-soluble impurities and residual agar. Finally, the purified material was dried to constant weight. Yields were expressed as the biopolymer weight percentage relative to the initial substrate, and results were reported as mean ± standard error (n = 3).

2.4. Characterization of the Different Biopolymers

2.4.1. Macroscopic and Microscopic Morphological Characterization

Macroscopic colony morphology of *A. luteoalbus* was evaluated on solid culture media formulated with different carbon sources by visual inspection throughout incubation. Colony characteristics, including mycelial density, surface texture, margin definition, and pigmentation, were recorded at 3 and 11 weeks of incubation to assess substrate-dependent morphological variation.

Microscopic characterization was performed to examine vegetative and reproductive structures. Fungal material was aseptically collected from the colony surface and mounted in lactophenol cotton blue. Observations were made with a light microscope at 40× and 100× magnification. Hyphal morphology and conidiogenous structures were evaluated and compared with published taxonomic descriptions of the genus *Acrostalagmus* to support the strain's morphological characterization.

2.4.2. Scanning Electron Microscopy (SEM)

To evaluate the microscopic morphology of the biopolymers, samples were pre-dried to remove residual moisture, mounted onto aluminum stubs with conductive carbon tape, and sputter-coated with a thin gold (Au) layer to enhance surface conductivity and minimize charging during observation. SEM images were acquired using a JEOL JSM-6010LA scanning electron microscope under the following conditions: accelerating voltage of 15 kV, working distance of 17 mm, and beam current of 41. Micrographs were taken at 2500× magnification with a 10 μm scale bar to compare morphological features among samples from different growth stages.

2.4.3. Preliminary Qualitative Screening of Thermal Behavior and Solubility

Thermal behavior was qualitatively assessed using a Fisher–Johns hot-stage apparatus by recording the onset temperature of softening/phase transition (upper limit: 250 °C). Since no complete melting was observed within this range, the apparent melting point was reported as >250 °C. Combustion/charring behavior was evaluated by direct flame exposure of standardized sample portions, and qualitative descriptors were recorded (ignition persistence, color change, odor, char/ash formation, and dripping behavior, if present). Solubility was assessed by adding 50 mg of biopolymer to 1 mL of each solvent (water, DMSO, 2-propanol, toluene, hexane, xylene, CCl_4, chloroform, ethyl acetate, and acetone), and dissolution was visually scored under the same conditions.

 doi:10.20944/preprints202606.0282.v1

2.4.4. Elemental Analysis (CHNS)

Elemental composition (C, H, N, and S) was determined in duplicate using a PerkinElmer PE2400 analyzer. Approximately 2 mg of each sample was analyzed at a combustion temperature of 975 °C and a reduction temperature of 501 °C, using helium as the carrier gas. Calibration was performed using cystine as the standard.

2.4.5. Thermal Analysis (TGA/DSC)

Thermal stability of the biopolymer was evaluated by thermogravimetric analysis (TGA) on a PerkinElmer TGA 4000 instrument. Samples were placed in alumina crucibles (70 µL) and heated from 30 to 550 °C at a heating rate of 10 °C/min under a nitrogen atmosphere. This temperature range allowed assessment of thermal degradation behavior and determination of the biopolymer's residual mass after thermal decomposition.

Differential scanning calorimetry (DSC) was performed on a Mettler Toledo DSC1 instrument (STAR software v14.0). Samples were placed in standard aluminum crucibles (40 µL), sealed, mechanically pierced, and heated from 30 to 550 °C at 10 °C/min under nitrogen atmosphere. This temperature range was selected to identify the main thermal transitions of the biopolymer, including glass transition and melting-related events.

2.5. Statistical Analysis

Statistical analysis was performed using GraphPad Prism software (version 10.3.1 for macOS). A one-way analysis of variance (ANOVA) was conducted specifically on the maximum biopolymer yield (Y_{max}) values to evaluate differences among the carbon sources. Tukey's multiple comparisons post hoc test was subsequently applied to identify specific pairwise differences between treatments. Statistical significance was established at $p < 0.05$.

3. Results and Discussion

3.1. Identification of the Microorganism Based on Macro- and Micromorphology

Morphological identification was carried out based on both macroscopic colony characteristics and microscopic structures. The colony morphology of *Acrostalagmus luteoalbus* grown on solid culture media containing different carbon sources and evaluated at distinct incubation times is shown in Fig. 1. The strain exhibited clear carbon source–dependent variations in colony pigmentation, surface texture, and mycelial density, which constitute relevant traits for morphological characterization and preliminary identification.

In particular, cultures grown on media containing complex carbon sources developed compact to cottony mycelia with well-defined pigmentation patterns, whereas the sucrose control showed reduced pigmentation and a more homogeneous colony appearance. These differences became more evident after prolonged incubation, as observed at 11 weeks compared with 3 weeks of cultivation (Fig. 1). Microscopic examination further confirmed the presence of characteristic conidiogenous structures consistent with the genus *Acrostalagmus*, supporting the morphological identification of the strain.

 doi:10.20944/preprints202606.0282.v1

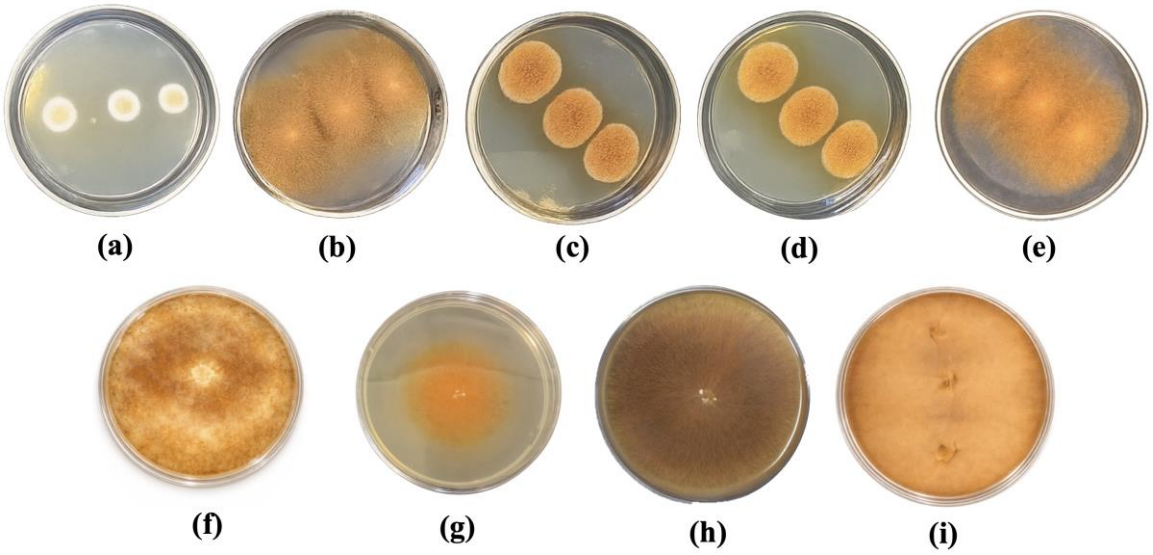

Figure 1. Macroscopic growth of *A. luteoalbus* on solid culture media containing different carbon sources. Substrate-dependent differences in mycelial density, colony surface texture, and pigmentation are observed. Images corresponding to 3 weeks of incubation are shown in panels (a–e): (a) corncob, (b) *Crataegus mexicana* (tejocote) pulp and peel, (c) banana peel, (d) orange peel, and (e) prickly pear peel. Panels (f–i) correspond to cultures after 11 weeks of incubation: (f) sucrose control, (g) orange peel, (h) prickly pear peel, and (i) *C. mexicana* pulp and peel.

Following the macroscopic characterization of colony morphology, the micromorphological features of *A. luteoalbus* were examined to further support strain identification. Representative microscopic structures observed after lactophenol cotton blue staining are shown in Fig. 2 (1000×).

Hyphae were hyaline, thin, and septate, forming a branched mycelial network. Conidiophores were erect structures bearing solitary or whorled phialides. Unicellular conidia were produced from these phialides and were generally ellipsoidal to sub-spherical, hyaline, and slightly curved. In the examined microscopic fields, conidia frequently occurred as compact aggregates at the tips of phialides, while abundant free conidia were also observed, indicating an active stage of sporulation.

The combination of these micromorphological traits, together with the macroscopic colony characteristics described above, is consistent with taxonomic descriptions of the genus *Acrostalagmus* and with previously reported characteristics of *A. luteoalbus*, thereby supporting the morphological characterization of the strain [35]. Overall, the macroscopic and micromorphological characteristics provide robust phenotypic support for the taxonomic placement of the isolate, which was subsequently confirmed by molecular identification based on ITS region sequencing.

 doi:10.20944/preprints202606.0282.v1

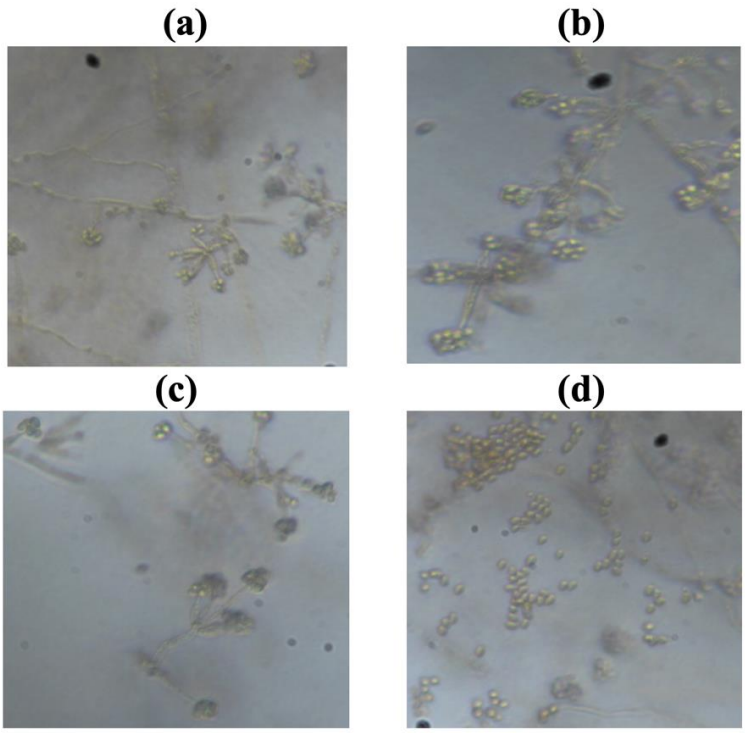

Figure 2. Microscopic morphology of *Acrostalagmus luteoalbus* stained with lactophenol cotton blue and observed by light microscopy (1000×). (a) Hyaline, thin, septate vegetative hyphae with early conidial aggregates. (b) Branched hyphae bearing solitary to whorled phialides with developing conidia. (c) Erect phialides producing compact clusters of ellipsoidal to sub-spherical conidia. (d) Abundant free conidia dispersed throughout the microscopic field, indicative of an active sporulation stage.

3.2. Molecular Identification

The taxonomic identity of the isolate was assessed by amplification and sequencing of the complete internal transcribed spacer (ITS) region (ITS1–5.8S–ITS2). A 611-bp amplicon was obtained, and the consensus sequence was compared against the NCBI database using BLASTn. The best match corresponded to *Acrostalagmus luteoalbus* (GenBank accession no. KT715723), with 100% sequence identity and 100% query coverage (E-value = 0.0). These metrics, together with the observed macro- and micromorphological traits, strongly support the identification of the isolate as *A. luteoalbus*. The sequence generated in this study was deposited in GenBank under accession no. PX916169.

3.3. Secretion of Extracellular Biopolymer by A. luteoalbus

Stereomicroscopic analysis revealed yellowish polymeric aggregates closely associated with the mycelial network of *A. luteoalbus* (Fig. 3). The material appeared as discrete, bright deposits on and adjacent to the hyphae, consistent with active extracellular secretion and progressive accumulation during solid-state cultivation.

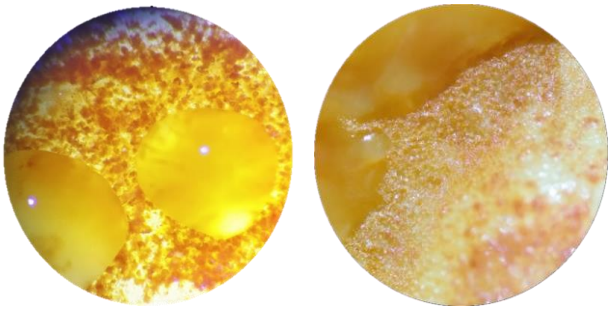

 doi:10.20944/preprints202606.0282.v1

Figure 3. Extracellular biopolymer produced by *A. luteoalbus* observed under a stereomicroscope (4×; BOECO, Germany, model BOE3200.001). Yellowish polymeric material appears as bright aggregates deposited on and around the mycelial network, consistent with extracellular secretion and accumulation.

3.4. Static Cultivation Showing Biopolymer Accumulation at the Air–Medium Interface

Under static cultivation, *A. luteoalbus* formed a thin and continuous polymer layer at the air–medium interface (Fig. 4) as the surface mycelium developed. This macroscopic pattern indicates sustained secretion and accumulation of extracellular material at the culture surface.

These observations are consistent with the stereomicroscopic evidence in Section 3.3 and are relevant to downstream processing. Because the product accumulates extracellularly, recovery can be performed with minimal biomass disruption, unlike intracellular systems such as polyhydroxyalkanoates (PHAs), which typically require cell-disruption-based extraction steps [24]. Quantitative data on the mass of the recovered polymer and comparative production yields for each substrate are provided in Section 3.5, Table 1, and Section 3.6, Figure 6.

Figure 4. Formation of a thin extracellular biopolymer layer at the air–medium interface during static cultivation of *A. luteoalbus* on a sucrose-based medium. The polymer is visible as a whitish surface film, consistent with extracellular secretion and accumulation, and facilitates subsequent recovery.

3.5. Effect of Substrate on Biopolymer Yield

The washed biopolymers obtained from each substrate are shown in Figure 5 after a three-hour reflux to remove residual agar and associated impurities.

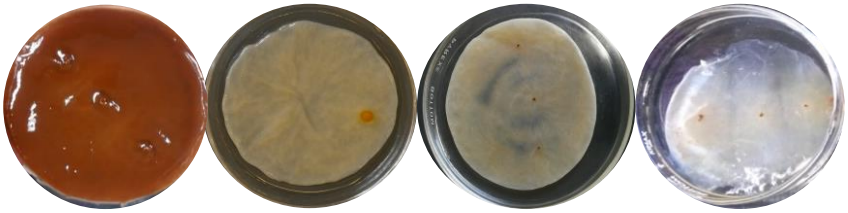

Figure 5. Washed biopolymers obtained after a three-hour reflux treatment for the removal of residual agar prior to drying and yield determination. Biopolymers were produced from different agro-industrial substrates, including tejocote (*C. mexicana*), and exhibited distinct macroscopic appearances after purification.

Following reflux, the materials were thoroughly washed and dried to constant weight, and the resulting biopolymer mass was recorded. Biopolymer yield was calculated using Equation 1.

$$\%\ \text{Biopolymer} = \frac{\text{Biopolymer mass (g)}}{\text{Substrate mass (g)}} \times 100 \qquad (1)$$

The kinetic parameters and maximum biopolymer yields ($Y_{p/s}$ ± standard error) for each substrate are summarized in Table 1. The results show that maximum biopolymer production was achieved at different incubation times depending on the substrate employed, confirming substrate-dependent production kinetics.

 doi:10.20944/preprints202606.0282.v1

Table 1. Kinetic parameters of extracellular biopolymer production by *Acrostalagmus luteoalbus* using different carbon sources.

Carbon Source	t_{max} (weeks) [1]	Y_{max} (%)[2]	Q_p (%/week)[3]
Tejocote pulp/peel	9	17.10 ± 1.29[a]	1.90
Sucrose	10	15.62 ± 0.77[a]	1.56
Prickly pear peel	10	10.15 ± 0.75[b]	1.02
Corncob	7	10.0 ± 0.45[b]	1.43
Banana peel	9	9.29 ± 0.63[b]	1.03
Orange peel	8	8.54 ± 1.13[b]	1.07

[1] t_{max}: incubation time to reach maximum yield. [2] Y_{max}: maximum biopolymer yield. [3] Q_P: volumetric productivity. Values for Y_{max} represent the mean ± standard error (n = 3). Different superscript letters (a, b) within the same column denote statistically significant differences according to a one-way ANOVA followed by Tukey's post hoc test ($p < 0.05$).

3.6. Effect of Substrate and Incubation Time on Biopolymer Yield

The data in Figure 6 show that all evaluated carbon sources supported biopolymer production, though yields varied markedly across substrate types and incubation times. Overall, biopolymer accumulation followed substrate-specific production kinetics, with clear differences in maximum yield and temporal profiles. Among the tested substrates, pulp with tejocote (*C. mexicana*) peel yielded the highest biopolymer content, reaching a maximum of 17.10% ± 1.29 at week 9. Although a slight decrease was observed by week 11 (15.86% ± 1.58), this substrate consistently outperformed the other residues throughout the fermentation period. These results identify week 9 as the optimal production point, suggesting that extended incubation beyond this point may increase operational costs without providing additional productivity benefits. Distinct yield patterns were observed across the remaining residues: corncob peaked at week 7 (10.00% ± 0.45), prickly pear peel at week 10 (10.15% ± 0.75), banana peel at week 9 (9.29% ± 0.63), and orange peel stabilized by week 4 and peaked at week 8 (8.54% ± 1.13). In contrast, the commercial sucrose control showed an almost linear increase through week 10, reaching a maximum of 15.62% ± 0.77.

Statistical analysis of the maximum yields (Y_{max}) confirmed these observations (Figure 6). One-way ANOVA ($F^{5,12} = 16.76,\ p < 0.0001$) followed by Tukey's post hoc test ($p < 0.05$) revealed that the maximum yield achieved with tejocote pulp and peel was statistically equivalent to the purified sucrose control (both assigned to Group a). Furthermore, both substrates significantly outperformed all other evaluated agro-industrial residues (Group b: prickly pear peel, corncob, banana peel, and orange peel), which exhibited no significant differences among themselves. This demonstrates that tejocote (*C. mexicana*) residue is a highly competitive, low-cost alternative to commercial carbon sources for biopolymer synthesis. Statistical analysis and kinetic parameters, including volumetric productivity (Q_P), are summarized in Table 1. Notably, the pulp with tejocote peel not only achieved the highest yield but also exhibited the highest productivity (1.90 %/week), reaching its maximum point faster and more efficiently than the sucrose control (1.56 %/week).

Several factors may explain the observed differences. Substrate composition plays a key role, as materials containing both pulp and peel likely provide higher levels of readily metabolizable sugars, minerals, and moisture, which favor fungal growth and biopolymer synthesis. Likewise, the accessibility of carbon sources directly influences polymer accumulation, with simpler, more bioavailable substrates promoting higher yields.

These findings align with previous reports highlighting agro-industrial residues, such as fruit peels and crop byproducts, as low-cost, carbon-rich substrates for microbial biopolymer production [36,37]. Nevertheless, reported yields are highly dependent on microbial strain, substrate pretreatment, and operational parameters including pH, temperature, and aeration [38,39]. For example, literature reports on intracellular bacterial biopolymers (such as PHAs) from agro-industrial wastes demonstrate extreme variability, with yields ranging from low baselines (<1%) to

 doi:10.20944/preprints202606.0282.v1

highly optimized accumulations exceeding 70% of the cell dry weight (CDW), depending on the specific organism and bioprocess [39].

In addition to chemical composition, the substrates' physical properties likely influenced production. Porous matrices facilitate oxygen transfer and nutrient diffusion, whereas denser materials may restrict mass transfer and reduce productivity. As is well-documented in the literature [40], the stabilization or decline in yields observed after weeks 10–11 is primarily driven by nutrient depletion. Furthermore, although not experimentally quantified in this study due to the static nature of the culture, the accumulation of secondary inhibitory metabolites and localized unfavorable pH shifts (common phenomena in prolonged, unbuffered fungal solid-state/static fermentations) is theoretically expected to contribute to this late-stage decline in polymer accumulation.

A particularly relevant finding of this study is that all biopolymers were produced extracellularly, regardless of the substrate used. During fungal growth, a thin polymer layer was consistently observed on the surface of the culture medium [41]. This extracellular localization offers significant technical advantages over intracellular polymer production by avoiding cell disruption and solvent-intensive recovery steps, thereby simplifying downstream processing and reducing production costs [42]. These advantages are especially important when using low-cost agricultural residues, where economic feasibility is closely tied to minimizing operational complexity [43]. Furthermore, the fact that yield curves for substrates like orange peel and corncob reached a stable plateau by week 6 or 7 suggests that the synthesized biopolymer is not susceptible to rapid enzymatic degradation by the host fungus after nutrient depletion.

Compared with the existing literature, baseline biopolymer yields from various agro-industrial residues are generally limited without extensive substrate pretreatment, enzymatic optimization, or substantial nutritional supplementation [44]. For instance, recent investigations evaluating fungal extracellular polysaccharide production under non-optimized solid-state fermentation report baseline mass yields that rarely exceed the 8–10% range, specifically ranging from 1.21% to 8.42% (12.1 to 84.2 mg/g substrate) depending on the biomass source [45]. In this context, the maximum yield of 17.10% ± 1.29 achieved with *C. mexicana* is particularly noteworthy. The convergence of this high yield, a high carbon content (44.50 ± 1.3%), significant thermal stability (T_{max} > 250 °C), and consistent macroscopic homogeneity across different carbon sources supports the presence of a robust and chemically resistant extracellular matrix. While this work represents an initial characterization, the integration of morphological, elemental, and thermal data provides a coherent and robust foundation that justifies the potential of *A. luteoalbus* as a promising alternative microbial platform.

In summary, these results demonstrate that substrate type critically affects biopolymer yield, that extracellular biopolymer production by *A. luteoalbus* offers clear technical and economic advantages, and that optimizing parameters such as pH, substrate concentration, and aeration could enhance productivity and product quality. However, because mechanical agitation in traditional shake flasks or stirred-tank bioreactors would disrupt the surface-associated polymer matrix and complicate downstream recovery, future scale-up efforts should focus on static systems, such as tray bioreactors. In these configurations, optimal aeration can be efficiently achieved through controlled headspace air exchange without disturbing the air–medium interface, thereby preserving the biopolymer's structural integrity and ease of recovery.

 doi:10.20944/preprints202606.0282.v1

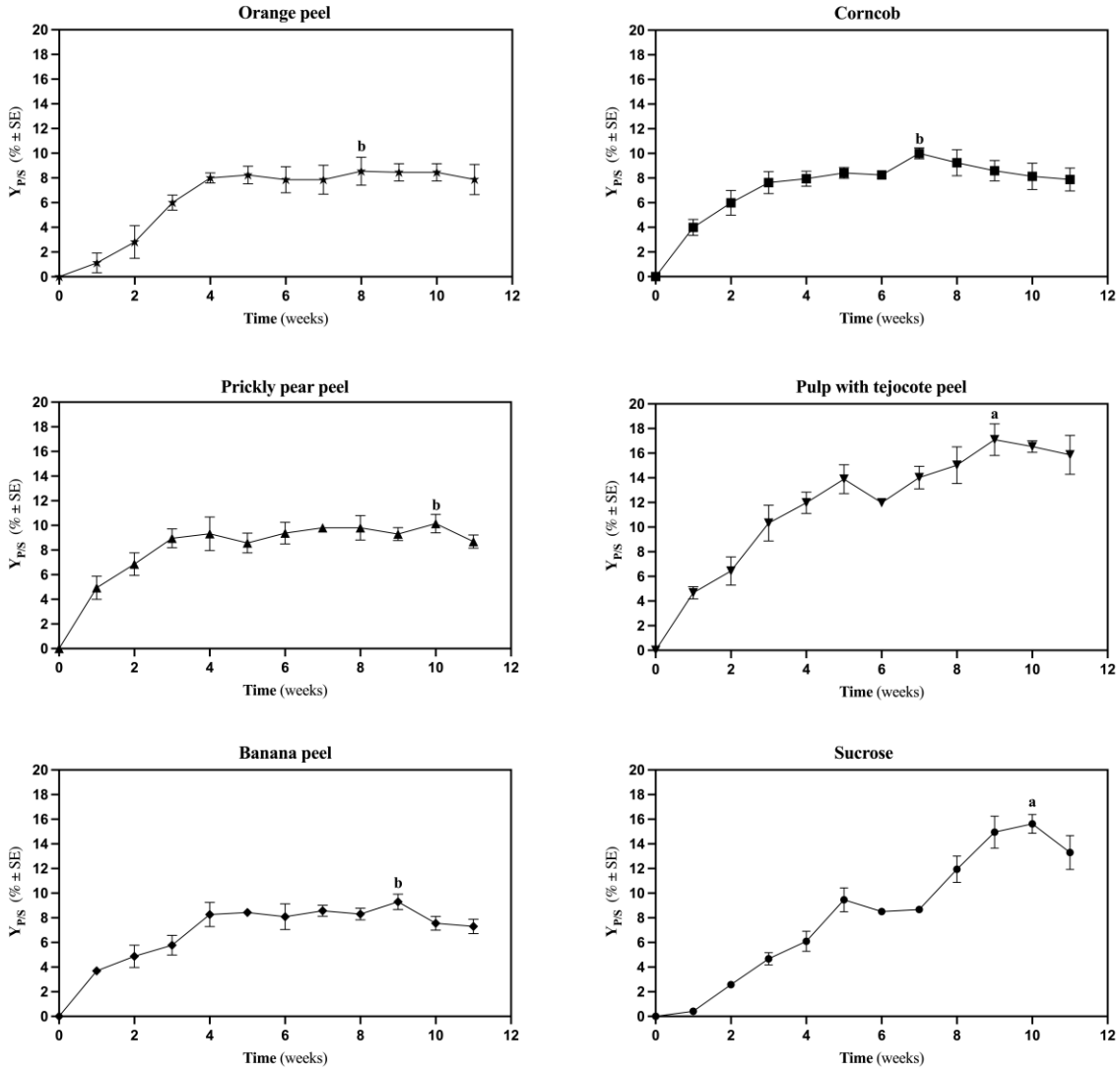

Figure 6. Average biopolymer yield ($Y_{P/S}$, % ± SEM) by *Acrostalagmus luteoalbus* obtained using different carbon sources over 11 weeks of fermentation. Substrates evaluated were orange peel, corncob, prickly pear peel, pulp with tejocote peel (*C. mexicana*), banana peel, and sucrose. Error bars represent the standard error of the mean (n = 3). Statistical analysis was performed exclusively on the maximum yield values (Y_{max}) achieved by each substrate. Different lowercase letters (a, b) placed above the maximum points denote statistically significant differences between treatments according to a one-way ANOVA followed by Tukey's post hoc test ($p < 0.05$).

3.7. Characterization of the Different Biopolymers

3.7.1. Scanning Electron Microscopy (SEM)

Scanning electron microscopy (SEM) was used to evaluate how substrate composition and fermentation time influence the microstructural development of the biopolymers. Analyses were performed on a JEOL JSM-6010LA microscope operating at an accelerating voltage of 15 kV and a working distance of 17 mm, with images acquired at magnifications from ×500 to ×2000.

The SEM micrographs (Figure 7) revealed a complex surface morphology. Substrates such as sucrose and tejocote pulp (*C. mexicana*) promoted the formation of relatively smooth, continuous, and compact surfaces, while materials derived from lignocellulosic residues showed irregular, amorphous, or fragmented morphologies. This structural configuration is of great interest in materials science, as the surface microarchitecture directly dictates how the polymer interacts with other matrices or biological systems. In this context, the morphological features observed by SEM are

 doi:10.20944/preprints202606.0282.v1

key determinants for proposing specific applications, ranging from high-performance biodegradable packaging to specialized scaffolds in biomedical engineering, where surface porosity and roughness are essential for functional performance [46]. These results suggest that substrates rich in metabolizable sugars favor homogeneous polymer deposition, whereas lignocellulosic residues may lead to incomplete organization and reduced structural cohesion.

The main microstructural features observed at both the initial and final fermentation stages are summarized in Table 2, which correlates morphological evolution with mechanical behavior and polymer yield. Substrates such as sucrose and tejocote peel pulp (*C. mexicana*) promoted the formation of uniform, mechanically resistant films during shorter fermentation periods, whereas corncobs and banana peels produced poorly organized or brittle structures that showed limited improvement over time. These results indicate that substrate composition directly affects both the kinetics of polymer formation and the structural integrity of the final material, consistent with previous studies [47,48].

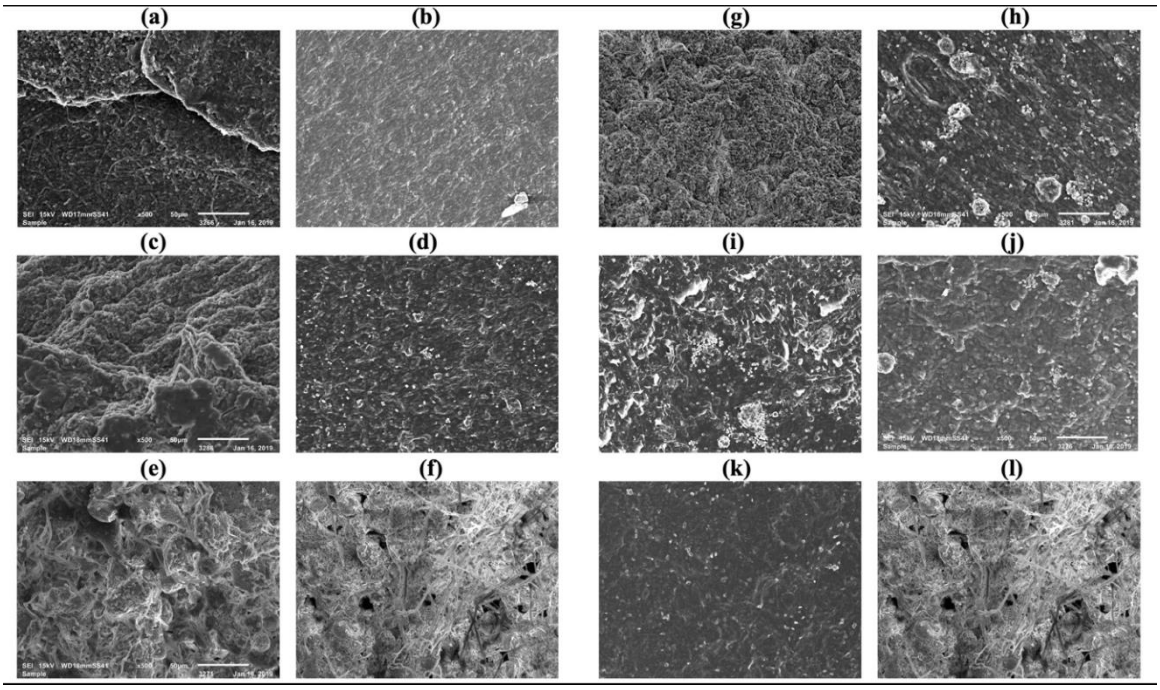

Figure 7. Scanning electron microscopy (SEM) micrographs of biopolymers produced from different substrates: (a, b) sucrose; (c, d) orange peel; (e, f) corncob; (g, h) banana peel; (i, j) prickly pear peel; (k, l) tejocote pulp with peel. Images were acquired at 15 kV, a working distance of 17 mm, magnifications of ×500–×2000, and a 50 μm scale bar.

Table 2. Comparative Summary relationship between substrate type, fermentation time, microstructural evolution, mechanical properties, and polymer yields.

Substrate	Initial Week	Initial Microstructure	Final Week	Final Microstructure	Mechanical Properties	Yield
Orange peel	7 weeks	Protuberances, partial transformation	10 weeks	Continuous, uniform film	High resistance	Medium
Corncob	5 weeks	Amorphous, poorly organized structure	10 weeks	Similar morphology, no major changes	Low resistance	Low
Prickly pear peel	5 weeks	Compact film	10 weeks	Brittle, fragmented structure	Reduced integrity over time	Medium

 doi:10.20944/preprints202606.0282.v1

Tejocote (*C. mexicana*) **peel pulp**	5 weeks	Fibrous, incomplete transformation	10 weeks	Continuous, uniform film	High resistance	High
Banana peel	7 weeks	Compact film	10 weeks	Fibrous, brittle structure	Reduced integrity over time	Medium
Sucrose	1 week	Scaly, compact structure	10 weeks	Thin, resistant, flexible film	High resistance & flexibility	High

The comparative analysis in Table 3 confirms that both substrate type and fermentation duration critically determine biopolymer microstructure, mechanical performance, and yield. Consistent with earlier reports [49,50], substrates containing simple sugars favored rapid polymer biosynthesis and the formation of continuous, mechanically robust films. In contrast, lignocellulosic substrates tended to yield polymers with lower cohesion and reduced mechanical resistance, likely due to slower carbon assimilation and heterogeneous metabolic pathways.

Compared with thermally processed synthetic polymers such as high-density polyethylene (HDPE), which typically exhibit dense, low-porosity structures associated with high mechanical strength and limited degradability [50], microbially synthesized polyhydroxyalkanoates (PHAs) are characterized by more amorphous, porous morphologies [46]. This intrinsic porosity, frequently reported in PHAs intended for biomedical and agricultural applications [51], enhances water uptake and molecular diffusion, properties that are advantageous for controlled-release systems and interactions with biological tissues. Moreover, the biodegradable nature and microbial origin of PHAs facilitate environmental and physiological degradation, supporting their growing use in regenerative medicine, smart packaging, and sustainable agricultural technologies [52,53].

3.7.2. Preliminary Qualitative Screening of Thermal Behavior and Solubility

The preliminary qualitative screening (Table 4) showed that the biopolymers obtained from all carbon sources shared similar macroscopic characteristics, including a dark brown color, an opaque appearance, a brittle texture, and a scratch-resistant surface. Using the Fisher–Johns method, no complete melting was observed up to 250 °C; therefore, the apparent melting point was recorded as >250 °C for all samples. While the biopolymer exhibits brittleness and generalized insolubility in common solvents, these properties suggest a highly cross-linked macromolecular network with high chemical resistance. Rather than a limitation for conventional plastic replacement, these characteristics position the *A. luteoalbus* biopolymer as a candidate for specialized applications, such as reinforcing fillers in biocomposites or functional coatings requiring high thermal stability, as the material remains stable above 250 °C.

In the combustion assay, the samples ignited with a red flame and a sweet odor. After the flame was removed, they exhibited whitening, an acrid odor, and ash formation, consistent with progressive carbonization. In the solubility panel, all samples were insoluble in the solvents tested (water, DMSO, 2-propanol, toluene, hexane, xylene, CCl_4, chloroform, ethyl acetate, and acetone), indicating high solvent resistance under the conditions tested. Overall, these qualitative observations suggest a chemically resistant and thermally robust matrix, potentially associated with dense intermolecular interactions, a high degree of crosslinking, and/or heterogeneous polymeric domains, as reported for other fungal-derived polymeric materials [54,55]. Moreover, the high thermal resistance (>250 °C), combined with generalized insolubility and progressive carbonization during combustion, is consistent with an extracellular biopolymer characterized by a compact macromolecular network and high carbon content [54]. Nevertheless, these tests constitute a preliminary screening and do not, by themselves, establish the monomeric composition or molecular architecture of the polymer, which requires complementary analytical techniques.

While the biopolymer exhibits brittleness and generalized insolubility in common solvents, these properties suggest a highly cross-linked macromolecular network with high chemical resistance. Rather than a limitation for conventional plastic replacement, these characteristics position the *A.*

 doi:10.20944/preprints202606.0282.v1

luteoalbus biopolymer as a candidate for specialized applications, such as reinforcing fillers in biocomposites or functional coatings requiring high thermal stability, as the material remains stable above 250 °C.

Table 3. Experimental results of physicochemical tests performed using different carbon sources.

Test performed	Result
Initial observations	Opaque, plastic-like appearance; brittle texture; scratch-resistant surface; dark brown color.
Apparent melting point (Fisher–Johns)	>250 °C (no complete melting observed up to 250 °C).
Combustion behavior	In flame: red flame, sweet odor, sustained ignition. After flame removal: whitening, pungent odor, and ash formation.
Solubility	Insoluble in water, dimethyl sulfoxide (DMSO), 2-isopropanol, toluene, hexane, xylene, carbon tetrachloride (CCl_4), chloroform, ethyl acetate, acetone.

3.7.3. Elemental Analysis (CHNS)

For structural and thermal characterization (CHNS, TGA, and DSC), the biopolymer derived from the commercial sucrose cultivation (at week 11) was selected as the analytical control. This methodological approach allowed for the elucidation of the intrinsic baseline structure and properties of the *A. luteoalbus* biopolymer, completely avoiding potential analytical noise or interferences from the complex heterogeneous matrices (e.g., residual pectins or lignocellulosic fragments) inherent to the agro-industrial substrates. Accordingly, elemental analysis (Table 4) of this representative sample revealed that the biopolymer contained 44.50 ± 0.13% carbon, 7.43 ± 0.13% hydrogen, 1.80 ± 0.03% nitrogen, and 0.61 ± 0.05% sulfur (mean ± SD, n = 2). The remaining mass fraction is most likely attributable to oxygen and other elements that are not quantified by CHNS and are not directly measured in this analysis.

The high carbon content, together with the comparatively low nitrogen and sulfur fractions, indicates a predominantly non-proteinaceous matrix and is consistent with complex, highly cross-linked polymeric structures enriched in carbohydrates. These values fall within the compositional ranges reported for fungal-derived extracellular polymeric materials [54,55] and align with the qualitative evidence of thermal robustness and solvent resistance discussed in the preceding section. Collectively, the CHNS results support the presence of a compact, carbon-rich macromolecular network characteristic of chemically resistant fungal biopolymers [56].

Nevertheless, CHNS analysis provides only the global elemental composition; therefore, specific structural assignment and detailed elucidation of the polymer architecture require complementary analytical approaches, such as monosaccharide profiling, spectroscopic techniques (e.g., FTIR and NMR), and molecular weight distribution analyses.

The elemental analysis revealed a nitrogen-poor composition (1.80 ± 0.03%), which is a critical finding. Fungal melanins [56] and complex humic-like substances typically exhibit significantly higher nitrogen content due to their indole-based or protein-rich precursors. Our results, showing low nitrogen and sulfur fractions, are more consistent with a non-proteinaceous, carbohydrate-rich, and highly cross-linked macromolecular matrix. This supports the hypothesis that the material is a specifically secreted extracellular biopolymer rather than a byproduct of mycelial aging or cell wall degradation.

 doi:10.20944/preprints202606.0282.v1

Table 4. Elemental analysis results obtained with the Perkin Elmer 2400 Elemental Analyzer.

Sample amount analyzed (mg)	% Carbon	% Hydrogen	% Nitrogen	% Sulfur
2.606	44.41	7.52	1.82	0.57
2.317	44.59	7.33	1.78	0.64
Mean ± SD (n=2)	44.50 ± 0.13	7.43 ± 0.13	1.80 ± 0.03	0.61 ± 0.05

3.7.4. Thermal Analysis (TGA and DSC)

Thermogravimetric analysis (TGA) (Table 5; Fig. 8) revealed a multistep mass-loss profile. Two early events at 35.71 °C and 54.77 °C accounted for a combined mass loss of 19.14%, attributable to the release of moisture and low-molecular-weight volatile components. The main thermal decomposition region occurred between approximately 250 and 400 °C, with maximum degradation rates at 286.20 °C, 316.84 °C, and 390.46 °C, indicating stepwise degradation of chemically distinct fractions within the polymeric matrix. At the end of the analysis, an estimated residual mass of ~27.23% was observed, consistent with the presence of thermally resistant domains.

Table 5. Thermogravimetric analysis (TGA) results obtained with the Perkin Elmer TGA4000.

Parameter	Result
Initial sample mass (mg)	**3.374**
T_{max}, stage 1 (°C)	35.710
Mass loss, stage 1 (%)	6.211
T_{max}, stage 2 (°C)	54.770
Mass loss, stage 2 (%)	12.929
T_{max}, stage 3 (°C)	286.200
Mass loss, stage 3 (%)	8.376
T_{max}, stage 4 (°C)	316.840
Mass loss, stage 4 (%)	28.017
T_{max}, stage 5 (°C)	390.460
Mass loss, stage 5 (%)	17.241
Total mass loss (%)	**72.774**
Estimated residual mass at 550 °C (%)	**27.226**

Note: T_{max} corresponds to the temperature of maximum mass-loss rate (DTG peak) for each stage.

 doi:10.20944/preprints202606.0282.v1

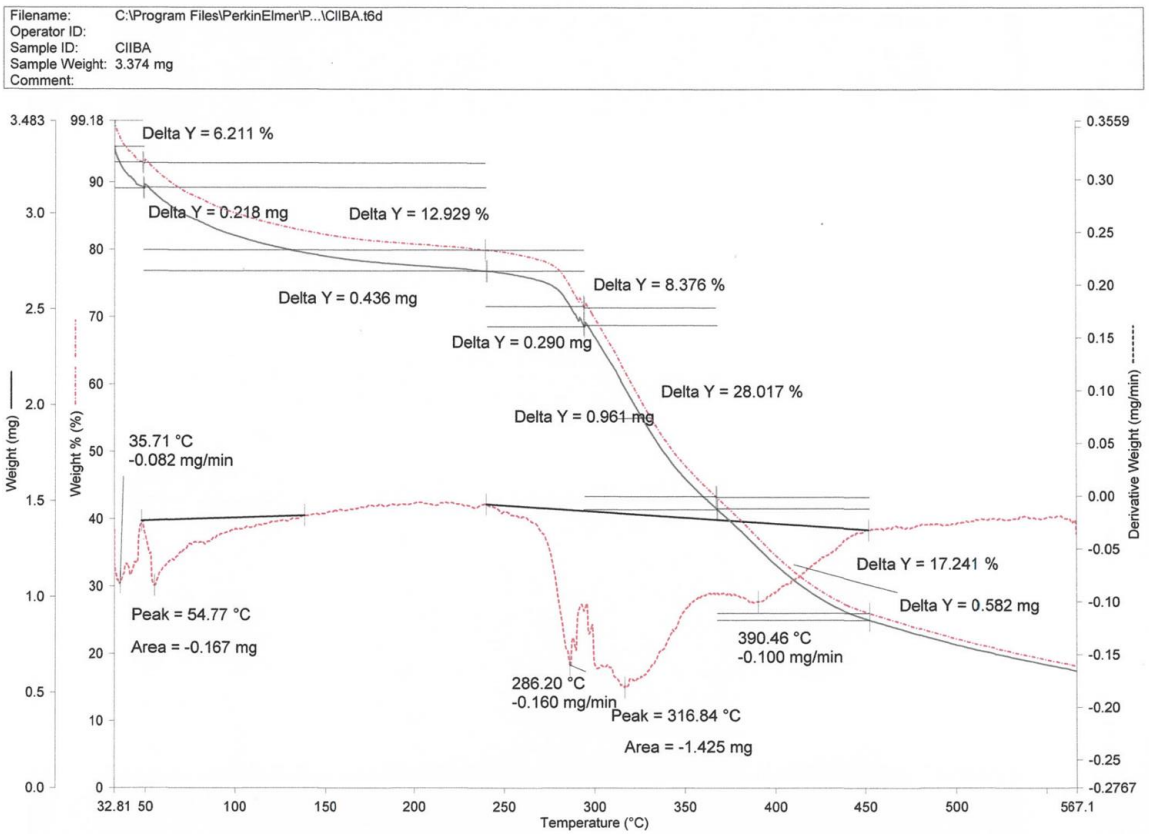

Figure 8. Thermogram obtained from thermogravimetric analysis (TGA). Mass percentage vs. temperature.

Differential scanning calorimetry (DSC) (Table 6; Figure 9) revealed multiple endothermic transitions, including low- and intermediate-temperature events as well as high-temperature events at 416.38 °C and 546.67 °C. A transition near 197.52 °C may correspond to a glass-transition-like event. Notably, no sharp melting endotherm characteristic of a well-defined crystalline fusion was detected before major thermal degradation. This behavior supports the presence of an amorphous or structurally heterogeneous material that undergoes progressive softening and decomposition rather than a discrete melting transition.

Table 6. Differential Scanning Calorimetry (DSC) results obtained with the Mettler Toledo DSC1.

Thermal event	Temperature (°C)	ΔH (J/g)	Tentative assignment
Low-temperature endothermic event (onset)	31.47		Moisture/volatile release
Low-temperature endothermic event (peak)	63.20	-260.07	Moisture/volatile release
Secondary endothermic event	84.52		Structural relaxation/rearrangement
Secondary endothermic event	123.82		Structural relaxation/rearrangement
T_g-like transition	197.52		Glass-transition-like behavior
Endothermic event	274.10		Pre-decomposition transition
Endothermic event	416.38		Thermal decomposition
Endothermic event	546.67		Advanced thermal decomposition

 doi:10.20944/preprints202606.0282.v1

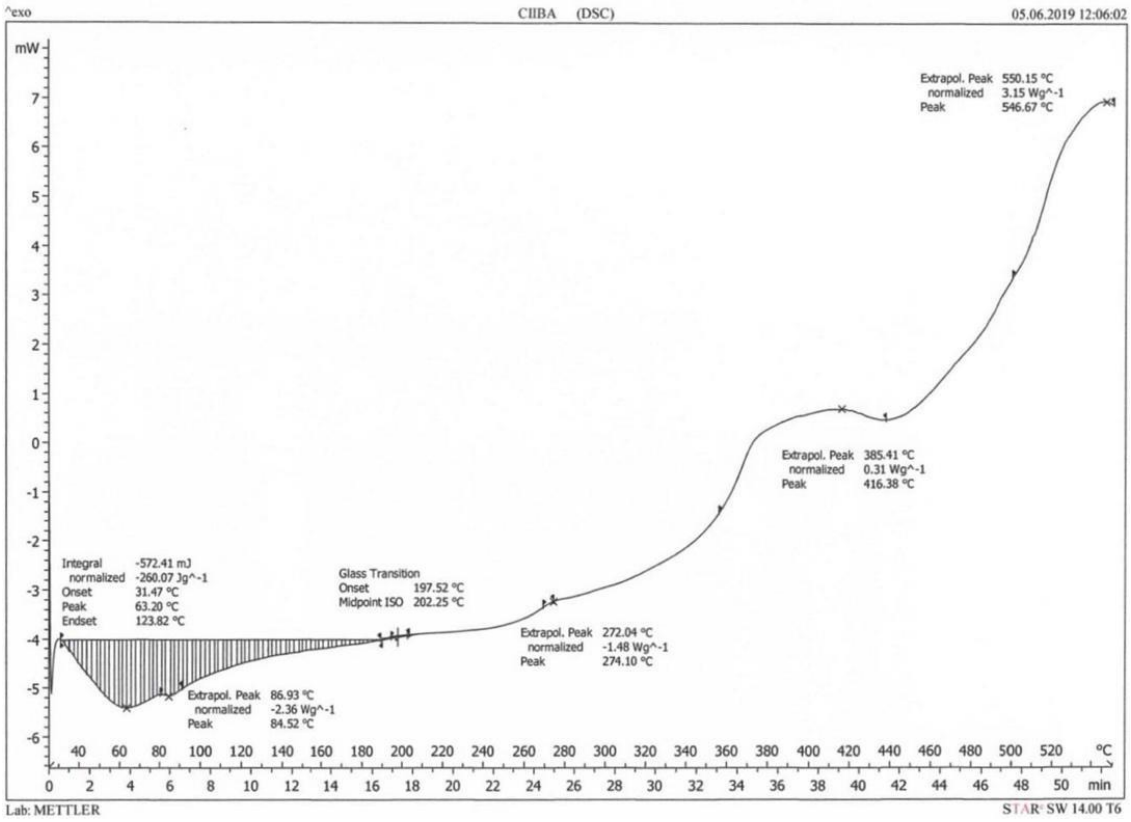

Figure 9. DSC thermogram of the sucrose-derived biopolymer (week 11): heat flow vs temperature (30–550 °C, 10 °C/min, N_2 atmosphere).

Overall, the combined TGA/DSC profiles support the presence of a thermally stable and structurally heterogeneous biopolymer, characterized by a compact macromolecular network and highly resistant domains, in agreement with the qualitative thermal screening and elemental composition analysis discussed in the preceding sections. Although thermal and CHNS analyses were conducted on the sucrose-derived sample, the consistency observed across macroscopic, elemental, and thermal properties suggests that the fundamental structural features described here are representative of the biopolymer obtained under the different carbon sources evaluated. Nevertheless, future comparative thermal analyses may further refine substrate-specific differences.

Taken together, the qualitative screening, elemental composition, and thermal analyses provide a coherent and robust characterization of the biopolymer produced by *A. luteoalbus*. The convergence of macroscopic homogeneity across carbon sources, high carbon content with low nitrogen and sulfur fractions, multistep thermal degradation, absence of a well-defined melting transition, and substantial residual mass collectively support the presence of a compact, non-proteinaceous, and structurally heterogeneous extracellular polymeric matrix. These features are consistent with fungal-derived biopolymers characterized by dense intermolecular interactions, carbohydrate-rich domains, and high thermal and chemical resistance.

Importantly, the agreement between qualitative observations and quantitative analytical data reinforces the internal consistency of the characterization approach employed. While further structural elucidation is required to fully resolve the monomeric composition and molecular architecture, the results presented here establish a solid physicochemical and thermal foundation for understanding the nature of the material and highlight its potential relevance for applications requiring stability under thermal and solvent-exposed conditions.

In this context, the characteristics of the biopolymer produced by *A. luteoalbus* can be directly compared with those of established microbial polymer platforms across processing parameters, solubility behavior, and thermal profile. From an operational perspective, a major limitation of bacterial polyhydroxyalkanoates (PHAs) is their intracellular accumulation, which requires cell

 doi:10.20944/preprints202606.0282.v1

disruption and solvent extraction for recovery, both of which represent a considerable share of downstream processing costs [42,43]. In contrast, the biopolymer produced by *A. luteoalbus* is secreted at the air–medium interface, enabling physical separation and reducing subsequent downstream unit operations [41].

Regarding solubility behavior, extracellular polymeric substances (EPS) synthesized by common fungal genera such as Aspergillus or Trichoderma possess carbohydrate-based backbones that render them water-soluble [41,45], but they often require post-synthesis chemical cross-linking to maintain their structural integrity in aqueous environments [41]. In contrast, the unmodified matrix produced by *A. luteoalbus* was insoluble across the evaluated panel of polar and nonpolar solvents and maintained its structural integrity without secondary chemical processing.

Finally, biodegradable thermoplastics such as polylactic acid (PLA) and bacterial poly(3-hydroxybutyrate) (PHB) exhibit thermal transitions at relatively low temperatures; PLA has a glass transition temperature (Tg ≈ 60 °C), whereas PHB has a narrow processing window because its melting temperature (Tm ≈ 175 °C) is close to its degradation temperature [46]. In contrast, the biopolymer produced by *A. luteoalbus* maintained its surface integrity without melting up to 250 °C, with its main decomposition events occurring between 250 and 400 °C. This thermal profile suggests thermoset-like behavior, supporting its technical feasibility for high-temperature functional coatings or as a filler in biocomposites, compared with standard microbial alternatives that typically undergo thermal transitions at lower temperatures.

4. Conclusions

This study demonstrates that *Acrostalagmus luteoalbus* represents a previously underexplored fungal platform for the extracellular biosynthesis of biopolymers using low-cost agro-industrial residues as carbon sources. Unlike the extensively reported *Aspergillus* derived biopolymers, *A. luteoalbus* exhibited a distinct production behavior characterized by extracellular polymer accumulation at the air medium interface, which significantly simplifies downstream recovery and reduces the need for solvent intensive extraction steps.

The results confirm that substrate composition and fermentation time are decisive parameters governing polymer yield and structural development. In particular, substrates rich in readily metabolizable sugars promoted faster polymer formation and the development of continuous, mechanically robust films, whereas lignocellulosic residues produced more heterogeneous, structurally weaker materials. These findings highlight a substrate-dependent structure–property relationship, contributing to a more detailed understanding of fungal biopolymer biosynthesis beyond well-studied genera such as *Aspergillus*.

Physicochemical, elemental, and thermal characterization revealed that the biopolymer produced by *A. luteoalbus* exhibits notable thermal stability, chemical resistance, and insolubility in common solvents. Importantly, these properties were achieved without post-synthetic thermal or chemical modification, distinguishing this material from many conventional fungal and bacterial biopolymers that require additional processing to attain comparable stability.

While the present study does not aim to fully define application-specific performance, the combination of extracellular production, thermal resistance, and substrate-driven tunability suggests that *A. luteoalbus*-derived biopolymers may represent a promising alternative within the broader family of microbial biopolymers. Future work should focus on molecular-level structural elucidation, mechanical optimization, and application-oriented testing to further position this material relative to established fungal and bacterial biopolymer systems.

This study constitutes the first scientific evidence of biopolymer production by *Acrostalagmus luteoalbus*. While further structural elucidation through advanced techniques like NMR or mass spectrometry will be necessary to fully resolve the monomeric architecture, the exhaustive physicochemical characterization provided here establishes a robust baseline. We are intentionally opening a new research path for this species, demonstrating that its metabolic plasticity can be harnessed for sustainable material development from agro-industrial waste.

 doi:10.20944/preprints202606.0282.v1

5. Perspectives

Future research should prioritize the detailed chemical elucidation of the biopolymers produced by *A. luteoalbus*, particularly at the level of their monomeric building blocks. Determining the specific carbohydrate units, aromatic components, or other structural motifs that constitute the polymer backbone is essential to accurately classify the material within existing families of fungal biopolymers and to distinguish it from polymers derived from related genera such as *Aspergillus*.

Compositional analysis using complementary techniques—including monosaccharide profiling, advanced spectroscopic methods (FTIR and NMR), and chromatographic approaches—will be necessary to establish how substrate composition influences polymer chemistry. Such analyses would also enable a clearer correlation between monomeric composition, microstructural organization, and the observed mechanical and thermal properties.

In parallel, further optimization of culture parameters (e.g., pH, carbon source concentration, and oxygen availability) should be conducted to assess their impact on both polymer yield and chemical composition. Furthermore, although prior acid hydrolysis of substrates provides readily fermentable sugars, identifying and quantifying the enzymatic profiles secreted by *A. luteoalbus* (e.g., specific hydrolases required to metabolize remaining oligosaccharides) is a crucial next step. Together, these studies would provide the mechanistic understanding required to position *A. luteoalbus* derived biopolymers within the broader landscape of microbial polymers and to support future application-oriented research without extending beyond the scope of the present findings.

Author Contributions: All authors contributed equally to writing the article. Additionally, all authors have reviewed and approved the final version for publication.

Funding: No funding was received for this study.

Institutional Review Board Statement: Not applicable.

Informed Consent Statement: Not applicable.

Data Availability Statement: The data presented in this study are available within the article. The nucleotide sequence generated in this study has been deposited in GenBank under accession number PX916169.1.

Acknowledgments: We thank Hugo Cuatecontzi-Flores and Alejandra Sánchez-Barrera for their technical support. Also, the authors thank Ramón Maruri-Gómez for language revision.

Conflicts of Interest: The authors declare no conflict of interest.

Abbreviations

The following abbreviations are used in this manuscript:

ANOVA	Analysis of variance
BLASTn	Basic Local Alignment Search Tool (nucleotide)
CHNS	Carbon, hydrogen, nitrogen, and sulfur analysis
CO_2	Carbon dioxide
CH_4	Methane
DMSO	Dimethyl sulfoxide
DSC	Differential scanning calorimetry
DTG	Derivative thermogravimetry
EPS	Exopolysaccharides
FTIR	Fourier transform infrared spectroscopy
ITS	Internal transcribed spacer
NCBI	National Center for Biotechnology Information
NMR	Nuclear magnetic resonance
PDA	Potato dextrose agar
PHA	Polyhydroxyalkanoate
PHB	Poly(3-hydroxybutyrate)

 doi:10.20944/preprints202606.0282.v1

PLA	Polylactic acid
PCL	Poly(ε-caprolactone)
PET	Polyethylene terephthalate
Q_P	Volumetric productivity
SDA	Sabouraud dextrose agar
SEM	Scanning electron microscopy
SD	Standard deviation
SE	Standard error
TGA	Thermogravimetric analysis
T_g	Glass-transition temperature
T_{max}	Temperature of maximum mass-loss rate
t_{max}	Incubation time to reach maximum yield
UV	Ultraviolet
$Y_{P/S}$	Biopolymer yield
Y_{max}	Maximum biopolymer yield

References

1. Schneiderman DK, Hillmyer MA. 50th Anniversary Perspective: There Is a Great Future in Sustainable Polymers. Macromolecules 2017;50:3733–49. https://doi.org/10.1021/acs.macromol.7b00293.
2. UNEP. Plastic Pollution 2022. https://www.unep.org/plastic-pollution (accessed October 5, 2025).
3. Ritchie H, Samborska V, Roser M. Plastic Pollution. Our World in Data 2023.
4. Organisation for Economic Co-operation and Development (OECD). Plastics. OECD 2022. https://www.oecd.org/en/topics/plastics.html (accessed October 5, 2025).
5. Hale RC, Seeley ME, La Guardia MJ, Mai L, Zeng EY. A Global Perspective on Microplastics. Journal of Geophysical Research: Oceans 2020;125:e2018JC014719. https://doi.org/10.1029/2018JC014719.
6. Wright SL, Kelly FJ. Plastic and Human Health: A Micro Issue? Environ Sci Technol 2017;51:6634–47. https://doi.org/10.1021/acs.est.7b00423.
7. Verma R, Vinoda KS, Papireddy M, Gowda ANS. Toxic Pollutants from Plastic Waste- A Review. Procedia Environmental Sciences 2016;35:701–8. https://doi.org/10.1016/j.proenv.2016.07.069.
8. Chamas A, Moon H, Zheng J, Qiu Y, Tabassum T, Jang JH, et al. Degradation Rates of Plastics in the Environment. ACS Sustainable Chem Eng 2020;8:3494–511. https://doi.org/10.1021/acssuschemeng.9b06635.
9. Ward CP, Reddy CM. We need better data about the environmental persistence of plastic goods. Proceedings of the National Academy of Sciences 2020;117:14618–21. https://doi.org/10.1073/pnas.2008009117.
10. Dutta D, Sit N. A comprehensive review on types and properties of biopolymers as sustainable bio-based alternatives for packaging. Food Biomacromolecules 2024;1:58–87. https://doi.org/10.1002/fob2.12019.
11. Baranwal J, Barse B, Fais A, Delogu GL, Kumar A. Biopolymer: A Sustainable Material for Food and Medical Applications. Polymers 2022;14:983. https://doi.org/10.3390/polym14050983.
12. Pugazhendhi A, Indira K, Jacob JM, Mukesh M, Kumar G. Biopolymers: Classification and Applications. Handbook of Biopolymers, Jenny Stanford Publishing; 2018.
13. Rosenboom J-G, Langer R, Traverso G. Bioplastics for a circular economy. Nat Rev Mater 2022;7:117–37. https://doi.org/10.1038/s41578-021-00407-8.
14. Ritzen L, Sprecher B, Bakker C, Balkenende R. Bio-based plastics in a circular economy: A review of recovery pathways and implications for product design. Resources, Conservation and Recycling 2023;199:107268. https://doi.org/10.1016/j.resconrec.2023.107268.
15. Folino A, Karageorgiou A, Calabrò PS, Komilis D. Biodegradation of Wasted Bioplastics in Natural and Industrial Environments: A Review. Sustainability 2020;12:6030. https://doi.org/10.3390/su12156030.
16. Cakmak OK. Biodegradable Polymers—a Review on Properties, Processing, and Degradation Mechanism. CircEconSust 2024;4:339–62. https://doi.org/10.1007/s43615-023-00277-y.
17. Nakajima H, Dijkstra P, Loos K. The Recent Developments in Biobased Polymers toward General and Engineering Applications: Polymers that are Upgraded from Biodegradable Polymers, Analogous to

 doi:10.20944/preprints202606.0282.v1

Petroleum-Derived Polymers, and Newly Developed. Polymers 2017;9:523. https://doi.org/10.3390/polym9100523.

18. Jaffur N, Jeetah P, Kumar G. A review on enzymes and pathways for manufacturing polyhydroxybutyrate from lignocellulosic materials. 3 Biotech 2021;11:483. https://doi.org/10.1007/s13205-021-03009-x.
19. Avgoulas DI, Papaneophytou CP, Halevas EG, Velali EE, Pantazaki AA. Challenges for Utilizing Inexpensive Agro-Food Wastes for the Microbial Production of Polyhydroxyalkanoates. Microbial Bioprocessing of Agri-food Wastes, CRC Press; 2023.
20. Chouhan A, Tiwari A. Production of polyhydroxyalkanoate (PHA) biopolymer from crop residue using bacteria as an alternative to plastics: a review. RSC Adv 2025;15:11845–62. https://doi.org/10.1039/D4RA08505A.
21. Leong YK, Show PL. Biorefineries and Circular Economy in the Production of Second- and Third-Generation Bioplastics. Second and Third Generation Bioplastics, CRC Press; 2023.
22. Moradali MF, Rehm BHA. Bacterial biopolymers: from pathogenesis to advanced materials. Nat Rev Microbiol 2020;18:195–210. https://doi.org/10.1038/s41579-019-0313-3.
23. Mahapatra S, Banerjee D. Fungal exopolysaccharide: production, composition and applications. Microbiol Insights 2013;6:1–16. https://doi.org/10.4137/MBI.S10957.
24. Sharma VK, Shah MP, Parmar S, Kumar A. Fungi Bio-prospects in Sustainable Agriculture, Environment and Nano-technology: Volume 2: Extremophilic Fungi and Myco-mediated Environmental Management. Academic Press; 2020.
25. Oiza N, Moral-Vico J, Sánchez A, Oviedo ER, Gea T. Solid-State Fermentation from Organic Wastes: A New Generation of Bioproducts. Processes 2022;10:2675. https://doi.org/10.3390/pr10122675.
26. Selvam T, Rahman NMMA, Olivito F, Ilham Z, Ahmad R, Wan-Mohtar WAAQI. Agricultural Waste-Derived Biopolymers for Sustainable Food Packaging: Challenges and Future Prospects. Polymers 2025;17:1897. https://doi.org/10.3390/polym17141897.
27. Jørgensen H, Kristensen J, Felby C. Enzymatic conversion of lignocellulose into fermentable sugars: Challenges and opportunities. Biofuels Bioproducts and Biorefining 2007;1:119–34. https://doi.org/10.1002/bbb.4.
28. Barua S, Shome G, Dolai S, Sarwar J. Recent Findings and Advances in Sustainable Conversion of Lignocellulosic Waste to Bioplastic Precursors for a Circular Economy. In: Mukherjee G, Dhiman S, editors. Value Addition and Utilization of Lignocellulosic Biomass: Through Novel Technological Interventions, Singapore: Springer Nature; 2025, p. 295–334. https://doi.org/10.1007/978-981-96-2786-8_12.
29. Kučuk N, Primožič M, Knez Ž, Leitgeb M. Sustainable Biodegradable Biopolymer-Based Nanoparticles for Healthcare Applications. IJMS 2023;24:3188. https://doi.org/10.3390/ijms24043188.
30. Shi T, Wang H, Li Y-J, Wang Y-F, Pan Q, Wang B, et al. Genus Acrostalagmus: A Prolific Producer of Natural Products. Biomolecules 2023;13:1191. https://doi.org/10.3390/biom13081191.
31. Andersson (Aino) Maria A., Salo J, Mikkola R, Marik T, Kredics L, Kurnitski J, et al. Melinacidin-Producing Acrostalagmus luteoalbus, a Major Constituent of Mixed Mycobiota Contaminating Insulation Material in an Outdoor Wall. Pathogens 2021;10:843. https://doi.org/10.3390/pathogens10070843.
32. Adebayo-Tayo B. C. Optimization of growth conditions for mycelial yield and exopolysaccharride production by Pleurotus ostreatus cultivated in Nigeria. Afr J Microbiol Res 2011;5. https://doi.org/10.5897/AJMR11.328.
33. Grum-Grzhimaylo AA, Georgieva ML, Bondarenko SA, Debets AJM, Bilanenko EN. On the diversity of fungi from soda soils. Fungal Diversity 2016;76:27–74. https://doi.org/10.1007/s13225-015-0320-2.
34. Popa M, Tăușan I, Drăghici O, Soare A, Oancea S. Influence of Convective and Vacuum-Type Drying on Quality, Microstructural, Antioxidant and Thermal Properties of Pretreated Boletus edulis Mushrooms. Molecules 2022;27:4063. https://doi.org/10.3390/molecules27134063.
35. Nguyen TTT, Hee Lee S, Jeong Jeon S, Burm Lee H. First Records of Rare Ascomycete Fungi, *Acrostalagmus luteoalbus* , *Bartalinia robillardoides* , and *Collariella carteri* from Freshwater Samples in Korea. Mycobiology 2019;47:1–11. https://doi.org/10.1080/12298093.2018.1550894.

 doi:10.20944/preprints202606.0282.v1

36. Singh R, Das R, Sangwan S, Rohatgi B, Khanam R, Peera SKPG, et al. Utilisation of agro-industrial waste for sustainable green production: a review. Environmental Sustainability 2021;4:619–36. https://doi.org/10.1007/s42398-021-00200-x.
37. Ramos AS, Chavez-González ML, Iliná A, Hernández JLM, Aguilar CN. Agro-Industrial Wastes from Fruits, Vegetables, and Cereals: Potential Substrates for the Production of Value-Added Products for a Sustainable Future. Bioresources and Bioprocess in Biotechnology for a Sustainable Future, Apple Academic Press; 2024.
38. Mohammady EY, Elshobary M, Ashour M, Mohammady EY, Elshobary M, Ashour M. From Wastes to Resources: Sustainable Applications of Agro-Industrial Byproducts for a Greener Future. Circular Bioeconomy - Integrating Biotechnology and Sustainability for a Greener Planet, IntechOpen; 2025. https://doi.org/10.5772/intechopen.1010715.
39. Naitam MG, Tomar GS, Kaushik R, Singh S, Nain L. Agro-Industrial Waste as Potential Renewable Feedstock for Biopolymer Poly-Hydroxyalkanoates (PHA) Production n.d.
40. Zhou W, Colpa DI, Geurkink B, Euverink G-JW, Krooneman J. The impact of carbon to nitrogen ratios and pH on the microbial prevalence and polyhydroxybutyrate production levels using a mixed microbial starter culture. Science of The Total Environment 2022;811:152341. https://doi.org/10.1016/j.scitotenv.2021.152341.
41. Delattre C, Cabrera-Barjas G, Banerjee A, Rodriguez-Llamazares S, Pierre G, Dubessay P, et al. 17 - Production of fungal biopolymers and their advanced applications. In: Taherzadeh MJ, Ferreira JA, Pandey A, editors. Current Developments in Biotechnology and Bioengineering, Elsevier; 2023, p. 497–532. https://doi.org/10.1016/B978-0-323-91872-5.00001-6.
42. Bolla M, Pettinato M, Ferrari PF, Fabiano B, Perego P. Polyhydroxyalkanoates production from laboratory to industrial scale: A review. International Journal of Biological Macromolecules 2025;310:143255. https://doi.org/10.1016/j.ijbiomac.2025.143255.
43. Gundlapalli M, Ganesan S. Polyhydroxyalkanoates (PHAs): Key Challenges in production and sustainable strategies for cost reduction within a circular economy framework. Results in Engineering 2025;26:105345. https://doi.org/10.1016/j.rineng.2025.105345.
44. Astudillo Á, Rubilar O, Briceño G, Diez MC, Schalchli H. Advances in Agroindustrial Waste as a Substrate for Obtaining Eco-Friendly Microbial Products. Sustainability 2023;15:3467. https://doi.org/10.3390/su15043467.
45. Adimy Prakash Shoba Savariyar, Elshikh Mohamed S., Ali Mohammad Ajmal, Biji Gurupatham Devadhasan. Bioconversion of agro-residues to make extracellular polysaccharides in solid state fermentation via Trichoderma hamatum using response surface methodology: Antioxidant and α-glucosidase inhibitor activity 2024;19:8368–87. https://doi.org/https://doi.org/10.15376/biores.19.4.8368-8387.
46. Dalton B, Bhagabati P, De Micco J, Padamati RB, O'Connor K. A Review on Biological Synthesis of the Biodegradable Polymers Polyhydroxyalkanoates and the Development of Multiple Applications. Catalysts 2022;12:319. https://doi.org/10.3390/catal12030319.
47. Gumel AM, Annuar MSM, Heidelberg T. Growth kinetics, effect of carbon substrate in biosynthesis of mcl-PHA by Pseudomonas putida Bet001. Braz J Microbiol 2014;45:427–38. https://doi.org/10.1590/s1517-83822014000200009.
48. Singh Saharan B, Grewal A, Kumar P. Biotechnological Production of Polyhydroxyalkanoates: A Review on Trends and Latest Developments. Chinese Journal of Biology 2014;2014:802984. https://doi.org/10.1155/2014/802984.
49. Betlej I, Salerno-Kochan R, Krajewski KJ, Zawadzki J, Boruszewski P. The influence of culture medium components on the physical and mechanical properties of cellulose synthesized by kombucha microorganisms. BioRes 2020;15:3125–35. https://doi.org/10.15376/biores.15.2.3125-3135.
50. Niknezhad SV, Kianpour S, Jafarzadeh S, Alishahi M, Najafpour Darzi G, Morowvat MH, et al. Biosynthesis of exopolysaccharide from waste molasses using Pantoea sp. BCCS 001 GH: a kinetic and optimization study. Sci Rep 2022;12:10128. https://doi.org/10.1038/s41598-022-14417-1.

 doi:10.20944/preprints202606.0282.v1

51. Ben Abdeladhim R, Reis JA, Vieira AM, de Almeida CD. Polyhydroxyalkanoates: Medical Applications and Potential for Use in Dentistry. Materials (Basel) 2024;17:5415. https://doi.org/10.3390/ma17225415.
52. Guo W, Yang K, Qin X, Luo R, Wang H, Huang R. Polyhydroxyalkanoates in tissue repair and regeneration. Engineered Regeneration 2022;3:24–40. https://doi.org/10.1016/j.engreg.2022.01.003.
53. Paloyan A, Tadevosyan M, Ghevondyan D, Khoyetsyan L, Karapetyan M, Margaryan A, et al. Biodegradation of polyhydroxyalkanoates: current state and future prospects. Front Microbiol 2025;16. https://doi.org/10.3389/fmicb.2025.1542468.
54. Jones M, Bhat T, Kandare E, Thomas A, Joseph P, Dekiwadia C, et al. Thermal Degradation and Fire Properties of Fungal Mycelium and Mycelium - Biomass Composite Materials. Sci Rep 2018;8:17583. https://doi.org/10.1038/s41598-018-36032-9.
55. Wu T. Production and Characterization of Fungal Chitin and Chitosan n.d.
56. Eisenman HC, Casadevall A. Synthesis and assembly of fungal melanin. Appl Microbiol Biotechnol 2012;93:931–40. https://doi.org/10.1007/s00253-011-3777-2.